The Preendosomal Compartment Comprises Distinct Coated And Noncoated Endocytic Vesicle Populations

Steen H. Hansen,* Kirsten Sandvig,‡ and Bo van Deurs*

*Structural Cell Biology Unit, Department of Anatomy, The Panum Institute, University of Copenhagen, Blegdamsvej 3, DK-2200 Copenhagen N, Denmark; and ‡Institute for Cancer Research at The Norwegian Radium Hospital, Montebello, 0310 Oslo 3, Norway

Abstract. The transfer of molecules from the cell surface to the early endosomes is mediated by preendosomal vesicles. These vesicles, which have pinched off completely from the plasma membrane but not yet fused with endosomes, form the earliest compartment along the endocytic route. Using a new assay to distinguish between free and cell surface connected vesicle profiles, we have characterized the preendosomal compartment ultrastructurally. Our basic experimental setup was labeling of the entire cell surface at 4°C with Con A–gold, warming of the cells to 37°C to allow endocytosis, followed by replacing incubation medium with fixative, all within either 30 or 60 s. Then the fixed cells were incubated with anti-Con A–HRP to distinguish truly free (gold labeled) endocytic vesicles from surface-connected structures. Finally, analysis of thin (20–30 nm) serial sections and quantification of vesicle diameters were carried out. Based on this approach it is shown that the preendosomal compartment comprises both clathrin-coated and noncoated endocytic vesicles with approximately the same frequency but with distinct diameter distributions, the average noncoated vesicle being smaller (95 nm) than the average coated one (110 nm). In parallel experiments, using an anti-transferrin receptor gold-conjugate as a specific marker for clathrin-dependent endocytosis it is also shown that uncoating of coated vesicles plays only a minor role for the total frequency of noncoated vesicles. Furthermore, after perturbation of clathrin-dependent endocytosis by potassium depletion where uptake of transferrin is blocked, noncoated endocytic vesicles with Con A-gold, but not coated vesicles, exist already after 30 and 60 s. Finally, it is shown that the existence of small, free vesicles in the short-time experiments cannot be ascribed to recycling from the early endosomes.

ENDOCYTOSIS of plasma membrane constituents and of molecules from the environment is essential to eukaryote cells. Endocytosis is involved in diverse processes such as concentrative uptake of metabolites and carrier molecules, for instance LDL and transferrin (11), downregulation of growth factor receptors with tyrosine kinase activity (4, 52), antigen processing and presentation (13), as well as turn-over of resident plasma membrane constituents (2, 21). It is well established that many ligands and their transmembrane glycoprotein receptors are internalized via clathrin-coated pits and vesicles (receptor-mediated endocytosis), and the clathrin molecules together with associated proteins such as adaptins (2, 9, 26, 35, 39), as well as specific signal sequences in the cytoplasmic domain of the receptors (4, 23, 24, 27, 52), play key roles in the process. The main characteristic of endocytosis from clathrin-coated pits seems to be the efficiency by which some selected membrane molecules are concentrated in the pits while others are excluded, the coated pits thus acting as molecular filters (1). Plasma membrane, as well as bound molecules and solutes, may also be internalized in a clathrin-independent way. This has been approached in studies where the endocytic mechanism was analyzed morphologically by quantifying binding of labeled ligands to coated and noncoated domains of the plasma membrane (22, 34, 51). Recently some very unusual mechanisms of clathrin-independent internalization of molecules have been reported, leading either directly to the endoplasmic reticulum, bypassing the normal endosomal pathway (25), or to a sequestration just below the plasma membrane in invaginations which apparently never detach completely from the plasma membrane (45). In other experiments, the clathrin-dependent endocytosis was blocked efficiently by hypertonic solutions, potassium depletion, or acidification of the cytosol (17, 18, 28, 30, 36, 38, 47, 49). Nonetheless, uptake of fluid-phase markers and of ricin, which binds to cell surface receptors with terminal galactose, was only reduced to some extent (30, 36, 38, 47).

However, since the methods to selectively inhibit endocytosis involve nonphysiological conditions, objections may be raised against results obtained with these methods, and the existence of a clathrin-independent endocytic mechanism is therefore still a controversial issue deserving further attention (see references 2, 7, 12, 21, 44). In cells where both mechanisms of endocytosis have been reported to operate, one would expect the existence of two (or more) distinct populations of early endocytic, or preendosomal, vesicles

simultaneously. Preendosomal vesicle is used here as an operational term for endocytic vesicles that have pinched off completely from the plasma membrane but not yet fused with (preexisting) endosomes or with other vesicles to form endosomes. Obviously, detailed electron microscopical analysis of cells exposed to pulse-chase experiments using appropriate markers during the pulse and very short chase periods is required. In the present study, we have established a Con A–anti-Con A assay for short time endocytosis experiments and combined this with analysis of thin serial sections and quantification of vesicle diameters. In this way we have for the first time been able to visualize directly how the earliest steps in endocytosis involve two distinct, preendosomal vesicle populations with different size distributions. One population is the typical clathrin-coated, the other population is clearly noncoated (nonclathrin coated) and has a smaller mean vesicle diameter (95 nm) than the clathrin-coated vesicle population (110 nm).

Materials and Methods

Cell Culture

HEp-2 and A431 cells were maintained in Dulbecco's modification of Eagle's medium (No. 12-332-54, Flow Laboratories, Irvine, Scotland), containing 5% (HEp-2) or 10% (A431) fetal calf serum (No. 011-06290 M; Gibco Ltd., Paisley, Scotland) and 2 mM L-glutamine (No. 043 05030; Gibco Ltd.). T-47D cells were propagated in RPMI-1640 (No. 12-602-54; Flow Laboratories) supplemented with 10% FCS, 2 mM gluatamine and 8 μg/ml insulin (25 IU/mg; Hagedorn Research Laboratory, Gentofte, Denmark). For all cell types, cultures were grown in T-25 flasks or 24-well disposable trays (NUNC, Roskilde, Denmark) and used for experimentation at 50–80% confluency and 1 d after a change of the medium.

Biochemical Experiments

Effect of Con A on Fluid-Phase Endocytosis of Sucrose. HEp-2 cells grown in disposable trays were rinsed with ice-cold Hepes buffer and incubated with 0–10 μg/ml Con A (No. C2010; type IV; Sigma Chemical Co., St. Louis, MO) for 60 min on ice with or without the addition of 2 mM N-ethyl maleimide (NEM; Sigma Chemical Co.) during the last 10 min. Next, the cells were incubated with 8 μCi/ml, 540 mCi/mmol, [^{14}C]sucrose, for 20 min at 37°C, washed five times with ice-cold PBS, and incubated with 2 mg/ml protease (No. 5147, type XIV; Sigma Chemical Co.) for 60 min on ice. Finally, after centrifugation, the cell pellets were dissolved in 0.1 M KOH and the radioactivity was measured.

Effect of Potassium Depletion on Endocytosis of Con A and Transferrin. HEp-2 cells were depleted for potassium by first exposing them to hypotonic medium for 5 min at 37°C and then incubating them in a potassium-free buffer as earlier described (30). Endocytosis of ^{125}I-Con A was measured by removing the cell surface-bound lectin with α-methylmannoside. The cells were incubated for 10 min at 37°C in the presence of 0.1 M α-methylmannoside, washed three times in the same solution, and then dissolved in 0.1 M KOH before the radioactivity was measured. ^{125}I-Transferrin endocytosis was measured as previously described (6).

Con A–Anti-Con A Assay

Cells were chilled and rinsed with PBS (containing magnesium and calcium) at 4°C. The cultures were then incubated at 4°C for 120 min with 5 nm colloidal gold-labeled Con A (No. L-7390; Con A–gold; Sigma Chemical Co., St. Louis, MO), which had been dialyzed against PBS and diluted with PBS to an OD_{520} = 0.5 (1 ml/T-25) before use. After washing with PBS at 4°C, the cells were incubated for 30 or 60 s at 37°C. To warm the cells rapidly, 7.5 ml of 37°C PBS were added per T-25 flask and replaced once before immersing the flask in a 37°C water bath. The clock timer was started at the first exposure to 37°C PBS and the incubation was terminated by removal of warm PBS and addition of 5 ml ice-cold fixative consisting of 2% formaldehyde, 0.1% glutaraldehyde in 0.1 M phosphate buffer pH 7.2 to each T-25 flask which was immediately put on ice and subsequently transferred to a 4°C room for 30 min. Upon rinsing with PBS, fixed cultures were incubated with rabbit anti-Con A conjugated to horseradish peroxidase (No. P283; Dakopatts, Glostrup, Denmark) in a 1:20 dilution in PBS for 60 min at 22°C. The specificity of the Con A–gold label was assessed by inclusion of either 5 mg/ml free Con A (Sigma Chemical Co.) or 2 mg/ml methyl α-D-mannopyranoside (Sigma Chemical Co.) during the incubation with Con A–gold.

Transferrin Receptor Assay

Using 8 nm gold-conjugated monoclonal mouse-anti-transferrin receptor antibody B3/25 (kindly provided by Dr. Colin Hopkins, Department of Biochemistry, Imperial College of Science, Technology and Medicine, London) this assay was performed according to the protocol for the Con A–anti-Con A assay, except for the use of a different HRP-conjugated antibody: rabbit anti-mouse immunogloblulins/HRP (No. P260, Dakopatts).

Recycling Assay

Cultures were incubated for 15 min at 37°C with rabbit anti-Con A/HRP (P283), which before experimentation was (*a*) dialyzed against PBS, (*b*) supplemented with 10% normal rabbit immunoglobulin, and (*c*) diluted 1:4 (final dilution). The cultures were then transferred to 4°C, rinsed thoroughly with PBS, and subsequently incubated with Con A–gold for 120 min at 4°C, rinsed with PBS at 4°C, and incubated further for 60 s or 15 min at 37°C as described above. After fixation, the cultures were processed for electron microscopy.

Electron Microscopy

HRP was visualized with diaminobenzidine and H_2O_2 as previously described (16). Cells were pelleted by centrifugation, postfixed in 2% OsO_4, contrasted en bloc with 1% uranyl acetate, dehydrated, and embedded in Epon. Routinely, 40–50-nm sections were collected on mesh grids; for serial sectioning, 20–30-nm sections were sampled on slot grids. In any case sections were examined in a Jeol 100 CX electron microscope without further contrasting.

Quantification of Coated Vs. Noncoated Vesicle Frequency

At least 150 cell profiles for the 60-s chase and 300 cell profiles for the 30-s chase were analyzed in each of the two assays. Thus the data presented in Table I are based on more than 900 cell profiles. All material in a given Epon section was included, since it is not known whether the composition of the preendosomal vesicle population varies in different parts of the cell, e.g., the apical vs. the basal surface or the cell center vs. the cell processes. For the Con A–anti-Con A experiments, all vesicle profiles were counted and photographed (for the size distribution analysis). In the transferrin receptor assay, with 30-s chase, the first 78 vesicles were counted and photographed (for the size distribution analysis) and the remaining 92 simply counted as for the data obtained with 60-s chase.

Table I. Relative Frequency of Coated and Noncoated Vesicles after a 30- or 60-s Chase at 37°C

Assay	Total number of vesicles*	Coated vesicles	Noncoated vesicles
		%	%
30 s			
Con A–anti-Con A	166	40	60
Transferrin receptor	170	74	26
60 s			
Con A–anti-Con A	204	48	52
Transferrin receptor	252	70	30

*Approximately 300 and 150 cell profiles for the 30- and 60-s chase, respectively, were analyzed in each assay to obtain these data. Thus the frequency of vesicles (coated plus noncoated) per cell profile is ~0.6 for 30-s, and 1.5 for 60-s chase.

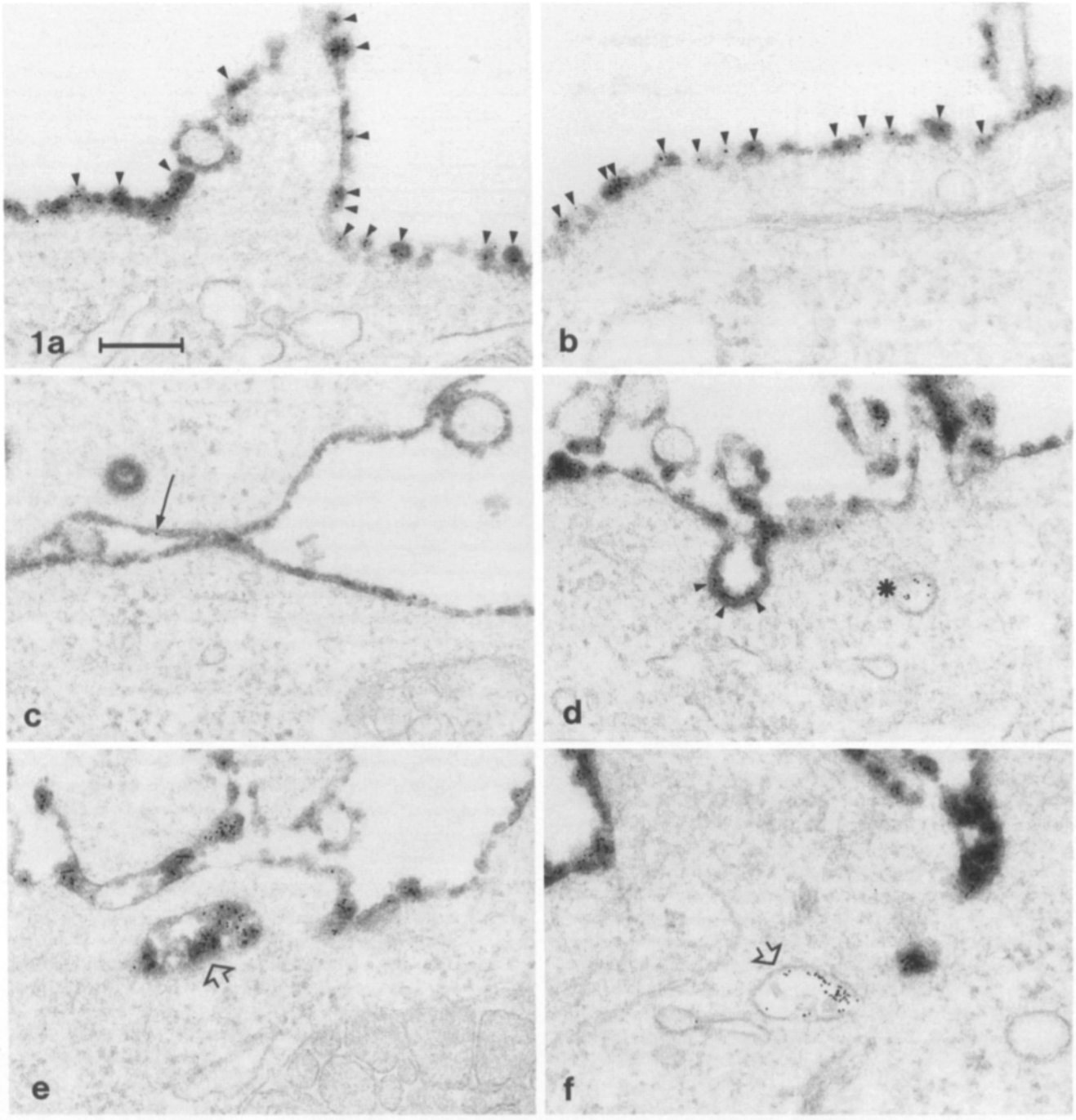

Figure 1. This figure shows technical aspects of the Con A–anti-Con A assay. HEp-2 cells (also used for all the following illustrations) were labeled with Con A–gold at 4°C, and then warmed to 37°C, and fixed within 60 s. Thereafter the cells were incubated with anti-Con A-HRP. *a* and *b* show how the Con A–gold complexes bind evenly to the cell surface and are surrounded by "clouds" of peroxidase reaction product (*arrowheads*). In *c* a control is shown where cells were incubated with Con A–gold in the presence of excess unlabeled Con A, followed by fixation and anti-Con A–HRP incubation as above. While gold labeling is very rare (*arrow*), HRP-labeling of the cell surface is distinct. *d* shows a surface pit with gold and HRP label (*arrowheads*) as well as free vesicle containing gold only (*asterisk*). *e* and *f* show two endosome-like profiles (*open arrows*). Only the one in *f* represents a free vesicle (only gold label) while that in *e* is surface connected as it contains both gold and HRP. Bar, 200 nm.

Determination of Vesicle Diameter Distributions

In the Con A–anti-Con A assay for 30- and 60-s chase, and in the transferrin receptor assay for 30-s chase, randomly selected sections of HEp-2 cells were examined in the EM at 16–26,000× and all vesicle profiles (coated or noncoated) containing only the gold label (see Results) (166 vesicles for the 30-s chase and 204 vesicles for the 60-s chase in the Con A–anti-Con A assay, and 78 vesicles for the 30-s chase in the transferrin receptor assay) were photographed at 26,000×. Micrographs were printed at a final magnification of 65,000×. Vesicle diameters, from center of membrane to center of membrane, thus excluding coat material, were measured with a Scale Lupe (a 0.1 mm scale mounted on 10× magnification glass) along a line drawn parallel to the baseline (the long, horizontal edge) of the print frame, and exactly at the same distance from the top and bottom of the vesi-

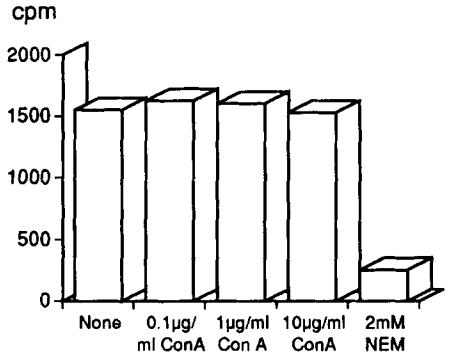

Figure 2. Endocytosis of the fluid phase marker ^{14}C-sucrose during a 20 min incubation at 37°C in cells which prior to the incubation had been exposed to the indicated concentrations of Con A for 60 min on ice in the presence or absence of 2 mM N-ethyl maleimide (NEM) during the last 10 min.

cle defined by two other lines drawn parallel to the baseline. Since the vesicles are randomly oriented in relation to the print frame, by measuring the diameters of the round or elongated vesicles in one dimension parallel to a predetermined edge of the print frame (the baseline), we obtain an accurate estimate of average diameters provided the number of measurements is adequate.

Results

The Con A–Anti-Con A Assay

Since newly formed endocytic vesicles are not possible to identify in routine preparations for the electron microscope, an appropriate marker system is needed. The marker should not be selective for specialized plasma membrane domains such as coated pits, but associate randomly with the entire cell surface. Moreover, a vesicular profile in a thin section containing label is not necessarily a free vesicle, but may be connected with the cell surface at another plane of sectioning. For instance, serial section analysis revealed that most (60–90%, depending on cell type) of the coated vesicular profiles containing cationized ferritin were actually surface connected (40). Finally, to focus on the earliest events in endocytosis, that is, the formation of the primary endocytic vesicles, termed preendosomal in the present study, very short incubation times are required.

We therefore established an assay making it possible to identify the preendosomal vesicles in the electron microscope. First, HEp-2 cells were incubated at 4°C with a Con A–gold conjugate in order to obtain a marked gold labeling of the entire cell surface. The cells were then allowed to internalize Con A–gold-tagged plasma membrane for very brief periods of time by replacing the cold medium with prewarmed medium at 37°C. After 30 or 60 s, this medium was rapidly replaced with ice-cold fixative and the cultures were immediately placed on ice. Hence the exact time in which the cells efficiently endocytosed Con A–gold is unknown, but it is definitely <30 and 60 s, respectively. Next, in order to distinguish truly internalized label (Con A–gold) from that associated with the cell surface including invaginations of the plasma membrane, which in a random section may appear as free vesicles, the fixed cells were incubated with anti-Con A antibody conjugated to HRP.

As shown in Fig. 1, Con A–gold particles bound to the plasma membrane and membrane invaginations are surrounded by a distinct cloud of dark HRP reaction product. In this way many coated or noncoated vesicular profiles or profiles resembling typical endosomes were found to be surface connected (Fig. 1). The HRP-labeled anti-Con A antibody clearly detected the Con A–gold even when this was localized in narrow spaces between adjacent cells or in structures connected with the cell surface by narrow "necks" or slits. By contrast, truly free (internalized) vesicles contained only the gold label (Fig. 1). This was further established by analysis of thin serial sections (see below) in the electron microscope, where a vesicular profile only containing gold label was found in the midsection of the series, and then followed on either side and photographed in all the sections. Hence, 32 vesicular profiles with gold label but without any HRP were analyzed in thin serial sections and in no case could any surface connection be detected. Furthermore, no vesicular profiles containing only gold label could be found, when the chase at 37°C was omitted.

The Con A–gold binding was specific. Hence, incubation with excess unlabeled Con A (5 mg/ml) in addition to the Con A–gold probe resulted in almost no gold labeling of the cell surface, whereas HRP reaction product due to the anti-Con A antibody was indeed very distinct (Fig. 1). Also, inclusion of methyl α-D-mannopyranoside (2 mg/ml) in the incubation step with Con A–gold almost completely prevented surface labeling both with gold and HRP.

To test whether Con A itself induced endocytosis, cells were incubated with increasing concentrations of prebound Con A at 37°C for 20 min and the effect on fluid-phase uptake on [^{14}C]sucrose was measured. As shown in Fig. 2, Con A does not induce any measurable endocytosis even within 20 min. Thus the endocytic processes described in the present paper are constitutive, not induced.

Characterization of Preendosomal Vesicle Populations

After 30 and 60 s of incubation, coated and noncoated endocytic vesicles of various size were observed, mainly in the peripheral cytoplasm (Figs. 3–6). Serial section analysis revealed that the noncoated vesicles (Figs. 5 and 6), like the coated ones, were spherical. The frequencies of coated and noncoated vesicles labeled with Con A–gold after 30- and 60-s chase at 37°C were roughly equal (Table I). The mean vesicle diameters (Tables II and III) suggested that the coated and noncoated vesicles were of similar size. However, the size distributions of the coated and noncoated vesicles shown in Figs. 7 and 8 revealed that this was not the case. It is seen that the noncoated vesicles tend to be smaller than the coated ones, both after 30 and 60 s. To test statistically whether the coated vesicle population was different from the noncoated population based on diameters, the two sets of data presented in Figs. 7 and 8 were analyzed by the Kolmogorov-Smirnov test. The test revealed that the difference between the diameter distributions of the two populations was significant with $P < 0.001$ and $P < 0.01$ for the 30- and 60-s chase, respectively. The main difference between the two time points is the increasing frequency of very large (>200 nm), uncoated vesicles after 60 s. If these vesicles, with a morphology of endosomes and with diameters above 200 nm, are omitted from the mean vesicle diameter calculation, the

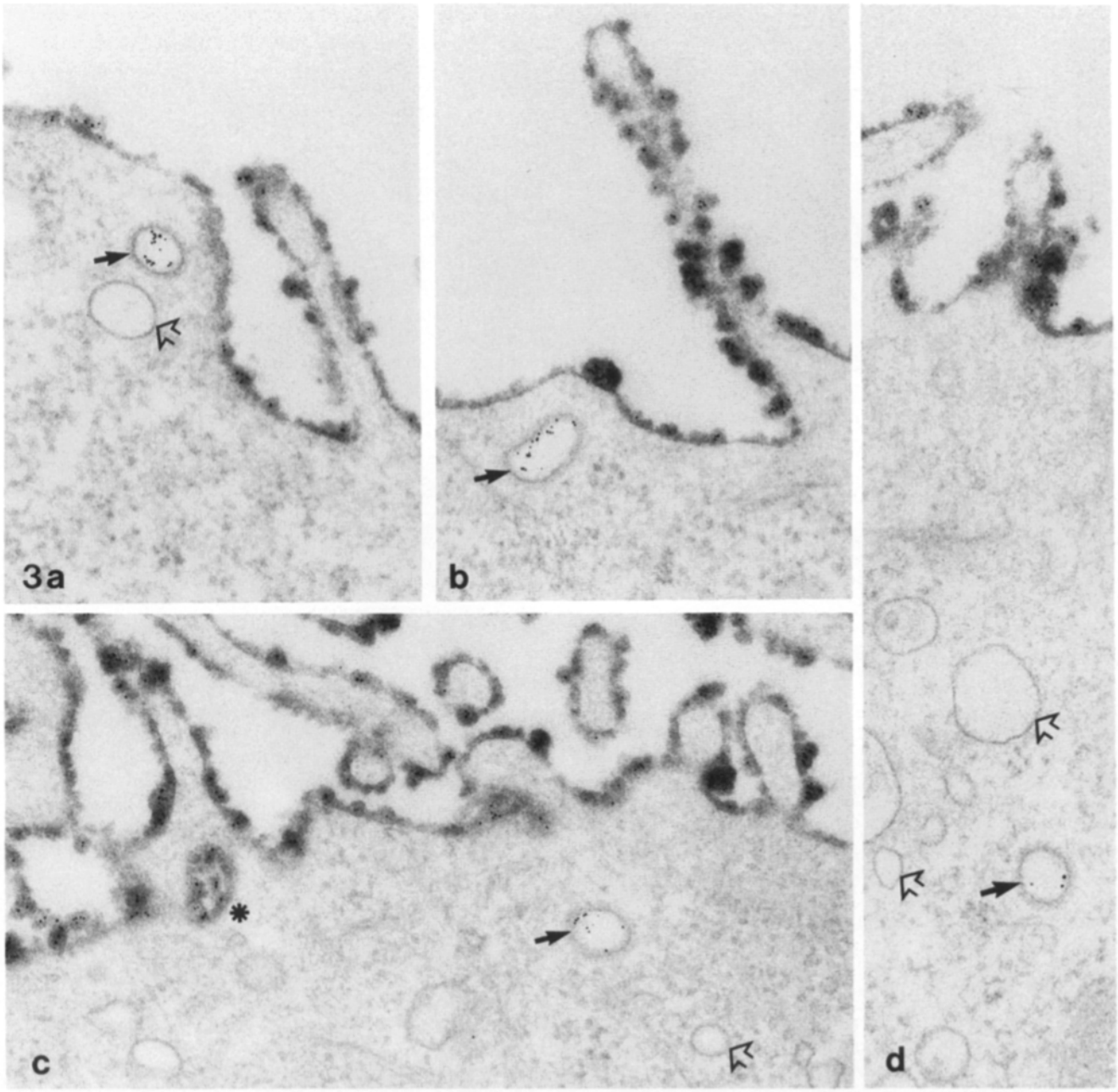

Figure 3. Cells were incubated with Con A–gold at 4°C, warmed to 37°C, and chased for 60 s. Then the cells were fixed and incubated with anti-Con A–HRP. Four examples of coated vesicles are shown (*arrows*). Noncoated vesicle profiles are shown in *a*, *c*, and *d* (*open arrows*) for comparison. Even in the low-contrast sections it is easy to distinguish between coated and noncoated vesicle profiles (see also Figs. 4–6). A surface-connected, vesicle-like profile is seen in *c* (*asterisk*).

characteristic smaller size of the noncoated vesicle type as compared to the coated one becomes evident (compare Tables II and III). Using the Mann-Whitney test for comparing the size of coated and noncoated vesicles, the difference was significant with $P < 0.0001$ and $P < 0.001$ for the 30- and 60-s chase, respectively. Thus the data indicate that the average diameter of the noncoated preendosomal vesicle is ~15 nm smaller than the coated one. It should be noted that the vesicle diameters in general are underestimated, since in a given section the largest diameter of a vesicle may not be included.

The Con A–anti-Con A assay was also applied to other cell types for 30- and 60-s intervals. Both in the human epidermoid carcinoma cell line A431 and in the human breast carcinoma cell line T47D, preendosomal vesicles (coated and noncoated) similar to those described above were present.

Uncoating of Clathrin-coated Vesicles

To test whether the noncoated vesicles in the 75–175-nm range (Figs. 7 and 8) were actually formed by pinching off from the plasma membrane without coat, or whether they

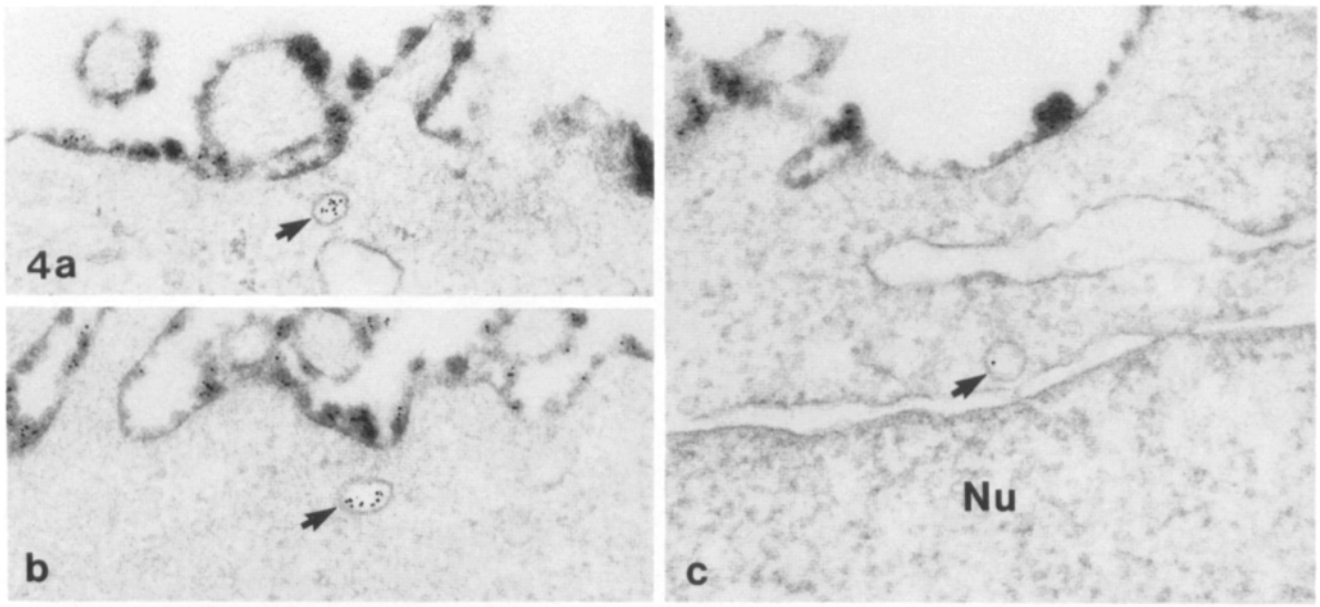

Figure 4. Three examples of noncoated vesicles (*arrows*) from an experiment similar to that in Fig. 3. *Nu*, nucleus.

represent previously coated vesicles which have shed the coat, we carried out experiments with monoclonal anti-transferrin receptor (TfR)[1]-gold. The TfR is a widely-used, bona fide marker of the coated pit pathway for endocytosis (19, 20, 47). When HEp-2 cells were prelabeled at 4°C with anti-TfR-gold and then warmed to 37°C and fixed within 30 s as described above, followed by incubation with rabbit anti-mouse/HRP to distinguish between truly free vesicles and surface-connected vesicles, 45 out of 170, or 26% (see Table I), of all free vesicles containing the gold label only were not coated. The ratio between uncoated and coated vesicle profiles in the transferrin receptor assay is thus ~1:3. Hence, since >50% of the vesicle profiles labeled with gold only in the Con A–anti-Con A assay were noncoated (Table I), maximally one-third of these are derived from coated vesicles. However, the one-third is most likely an overestimation of the role of vesicles "born" coated in the total noncoated vesicle frequency. It was striking that ~50% of the noncoated vesicles recorded in the transferrin receptor assay (Table III) were either large vacuoles (endosome-like) or small tubular structures (Fig. 9), which are unlikely to be formed simply by uncoating of coated vesicles. They rather represent endosomes, endosomal tubular extensions, and/or a few truly noncoated vesicles that by chance have internalized the transferrin receptor. Similar results for the transferrin receptor assay were obtained when the chase was prolonged to 60 s (Table I).

Since there was no significant difference between 30 s and 60 s in the frequency of uncoated vesicles (Table I), it is likely that a newly formed coated vesicle becomes uncoated within <30 s, and that the lifetime of an uncoated vesicle (i.e., before fusion with endosomes) is even shorter.

Inhibition of Coated Vesicles by Potassium Depletion

Studies by our group and others of HEp-2 cells have shown that K^+-depletion combined with a hypotonic shock (30, 36), as well as acidification of the cytosol (47), efficiently inhibits endocytosis of transferrin from coated pits by removing or paralyzing them, respectively. In contrast, ricin uptake is only moderately reduced. We therefore intended to analyze, using the Con A–anti-Con A assay described above, the preendosomal vesicle populations in cells where the coated pit pathway was blocked. Using HEp-2 cells, and because we wanted to eliminate the clathrin coats completely rather than paralyzing them, the K^+-depletion assay was chosen. Under the experimental conditions, the internalization of iodinated Con A during 20 min was reduced only from 22 to 13% (of total cell-associated Con A), whereas accumulation of sucrose was reduced to about one-third (36%) of the control. This was as expected because of the smaller volume-to-surface ratio of the noncoated vesicles as compared to coated vesicles. In contrast, uptake of transferrin during 15 min was reduced from 51 to 6% (data not shown). Thus, as in the case of ricin (30, 36, 47), Con A becomes internalized to a significant degree under conditions where uptake of transferrin is strongly reduced. With the Con A–anti-Con A assay applied to K^+-depleted cells, only noncoated, free vesicles with gold label and the same diameter range as described above were detected after 30- and 60-s chase (Fig. 10). However, K^+-depletion in combination with the necessary cooling step and brief (60 s) 37°C chase in the Con A–anti-Con A assay resulted in a 45% reduction in the number of noncoated vesicles.

These data indicate that the noncoated endocytic vesicles revealed with the Con A–anti-Con A assay under normal conditions also function in a situation where the coated pit pathway has been eliminated.

Recycling Vesicles

Previous studies have indicated that recycling vesicles (i.e., vesicles carrying membrane back to the plasma membrane from the endosomes-lysosomes) are small, <100 nm (53),

1. *Abbreviation used in this paper*: TfR, transferrin receptor.

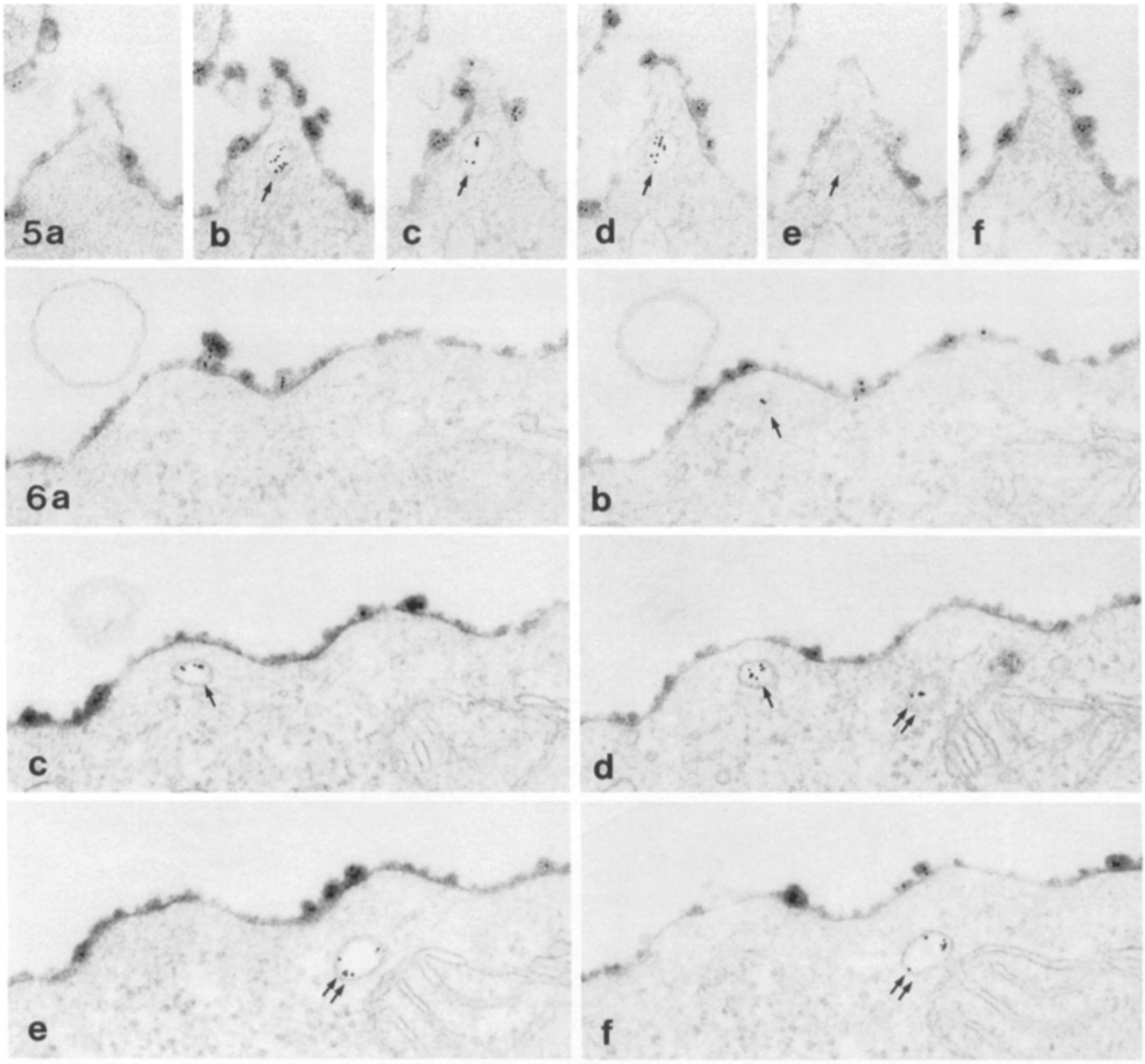

Figures 5 and 6. Two examples of noncoated vesicles as revealed by serial sectioning (*arrows* in Fig. 5, *b–e*, and Fig. 6, *b–d*), from an experiment similar to that in Fig. 3. In Fig. 6, *d–f* (*double arrows*) another noncoated vesicle is appearing.

thus of a size similar to that of the average putative noncoated preendosomal vesicle. Since we observed some internalized Con A–gold in endosome-like vesicles already after 30 s, we had to consider the possibility that part of the noncoated vesicle population shown in the histograms (Figs. 7 and 8) consisted of recycling vesicles rather than primary endocytic vesicles. To test this possibility, we reversed the sequence of reagents in the Con A–anti-Con A assay using the anti-Con A/HRP antibody first as a fluid-phase marker for 15 min at 37°C to label endosomes and recycling vesicles, followed by Con A–gold for 120 min at 4°C before the final chase at 37°C. Recycling vesicles containing the gold label can be distinguished from gold-labeled endocytic vesicles by their content of HRP. Under these conditions, with a 60-s chase, it was almost impossible to find the double-labeled recycling vesicles, although many gold-labeled coated and noncoated vesicular profiles were present in addition to endosomes containing significant amounts of HRP as well as gold particles (Fig. 11). After a 15-min chase at 37°C, when extensive colocalization of the gold and HRP label was present in

Table II. Average Size of Coated Vesicles in the Con A–Anti-Con A and Transferrin Receptor Assays

Assay	Chase	Number of coated vesicles measured	Vesicle diameter mean ± SD*
	s		*nm*
Con A–anti-Con A	30	66	114 ± 28
Con A–anti-Con A	60	97	108 ± 25
Transferrin receptor	30	58	108 ± 24

* Note that no coated vesicles with diameters above 175 nm were found, see Figs. 7 and 8.

Table III. Average Size of Noncoated Vesicles in the Con A–Anti-Con A and Transferrin Receptor Assays

Assay	Chase	Vesicle diameters above 200 nm included*		Vesicle diameters above 200 nm excluded*	
		Number of noncoated vesicles measured	Vesicle diameter mean ± SD	Number of noncoated vesicles measured	Vesicle diameter mean ± SD
	s		*nm*		*nm*
Con A–anti-Con A	30	100	104 ± 50	95	95 ± 30
Con A–anti-Con A	60	107	110 ± 57	97	95 ± 36
Transferrin receptor	30	20	126 ± 80	18	103 ± 36

* Based on the histograms shown in Figs. 7 and 8 it is assumed that vesicles with diameters above 200 mm represent endosomes. If such vesicles (5 in the 30s, and 10 in the 60s Con A–anti-Con A assay, and 2 in the transferrin receptor assay) are excluded from the calculation of mean diameters it becomes evident that the noncoated vesicles are distinctly smaller than the coated vesicles in Table II.

the endosome-like structures (Fig. 11), small double-labeled vesicular profiles could be detected, but their frequency was low. Thus the recycling assay devised in the present paper provides evidence that the contribution of recycling vesicles to the vesicle populations characterized by the Con A–anti-Con A assay was insignificant.

Discussion

In the present study we show that the preendosomal endocytic vesicle compartment contains two distinct vesicle populations: clathrin-coated vesicles ~110 nm in diameter, and noncoated (i.e., nonclathrin-coated) ~95 nm in diameter, both types of vesicles occurring with approximately the same frequency. This supports previous studies reporting that when endocytosis from clathrin-coated pits has been inhibited by K^+ depletion (30, 36) or acidification (47), ricin is still internalized at a rate of ~40–80% of the control value. Also, in the present study, uptake of Con A in K^+-depleted cells was ~59% of the control value. Evidence that (at least) two separate endocytic pathways exist is now based not only on biochemical studies using nonphysiological conditions,

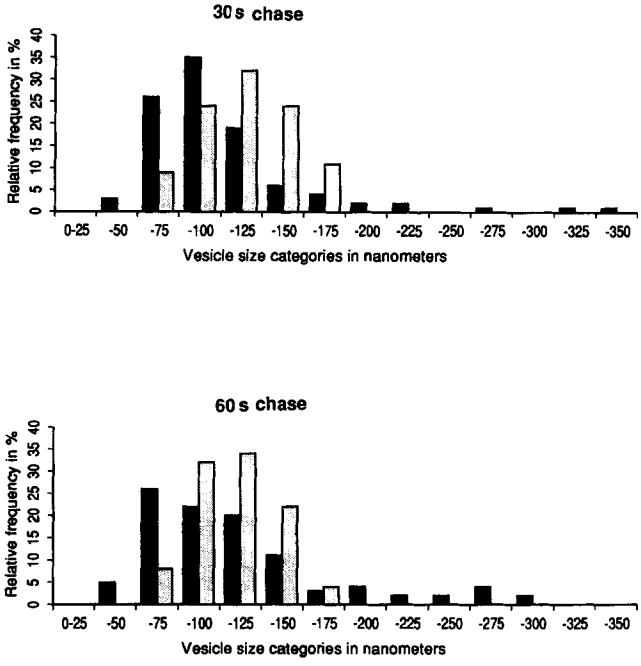

Figures 7 and 8. Histograms showing the diameter distributions of coated and noncoated vesicles obtained with the Con A–anti-Con A assay after chasing cells for 30 (Fig. 7) and 60 s (Fig. 8). 300 and 150 cell profiles were examined in the electron microscope for the 30- and 60-s chase, respectively, and all vesicle profiles containing only the gold label were photographed and printed at 65,000×. Vesicle diameter was measured on the print as described in Materials and Methods. The diameters of coated and noncoated vesicles were separately pooled in 25-nm categories and the frequency of vesicles in each category was calculated. (*Solid bars*) Noncoated; (*dotted bars*) coated.

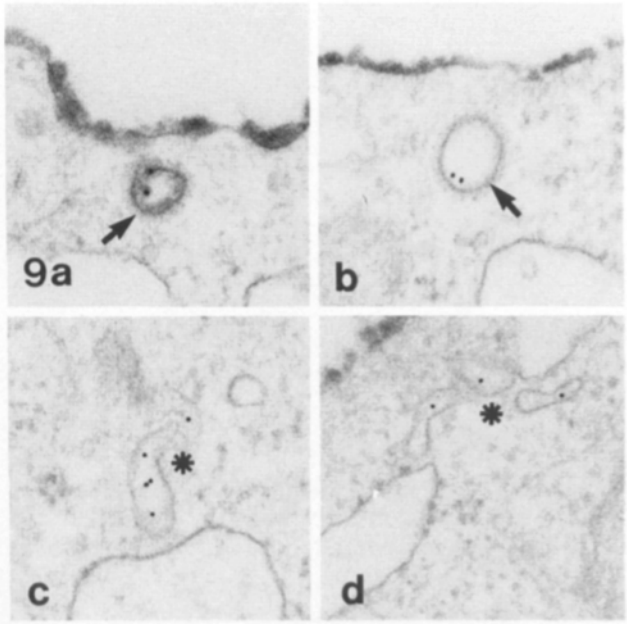

Figure 9. Cells incubated with anti-TfR–gold complexes and chased for 30 s at 37°C. After fixation, cell surface–associated anti-TfR–gold was detected using HRP-labeled rabbit anti–mouse immunoglobulins. In this assay, anti-TfR–gold-labeled coated pits appearing as vesicles (*arrow* in *a*) are also HRP labeled and thereby distinguished from true coated vesicles containing the anti-TfR–gold only (*arrow* in *b*). Although the majority of the gold labeled vesicles in this assay were coated, a heterogenous noncoated vesicle population encompassing larger vacuoles or small tubular structures (*c* and *d*) was also found.

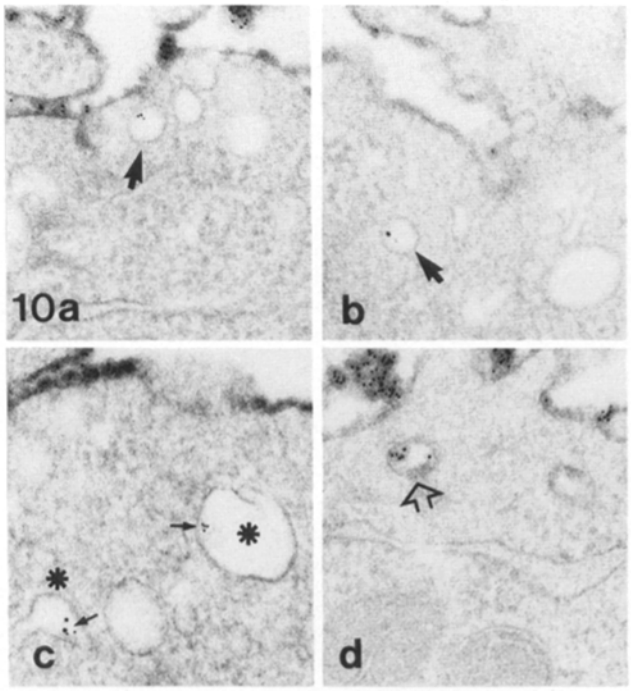

Figure 10. The Con A–anti-Con A assay applied to cells exposed to combined hypotonic shock and potassium depletion which is known to perturb clathrin dependent endocytosis. Noncoated (*arrows*) but not coated vesicles containing only gold are found under these conditions (*a* and *b*). Some larger vesicles (*asterisks* in *c*) are also gold labeled (*small arrows*). In *d* a surface-connected vesicular profile (*open arrow*) containing both HRP and gold is shown.

but also on quantitative morphological evidence obtained under nonperturbating conditions.

It is necessary to stress here the importance of the term "preendosomal" vesicle. It refers strictly to the newly formed endocytic vesicle, immediately after it has pinched off from the plasma membrane but before any fusion events (to give rise to early endosomes) have taken place. The study of such vesicles obviously requires short-time experiments, such as those reported here. For technical reasons we find it unwarranted to use shorter periods of incubation at 37°C than 30 s. On the other hand, if one incubates cells for 3–5 min (a typical short time interval in most studies on endocytosis), the ultrastructural pattern of smaller and larger vesicle profiles representing preendosomal vesicles, endosomes, and tubulo-vesicular processes from these, recycling vesicles, etc., becomes too complicated to allow any detailed analysis.

Since few endocytic vesicles are formed during a 30–60-s incubation at 37°C (see Table I), a marker molecule with a high number of cell surface binding sites is required. This requirement may not be essential when some of the proteins internalized selectively by the highly efficient coated pit pathway are studied, but it becomes absolute when the marker molecule must be nondiscriminative between different endocytic mechanisms. As our results show the Con A–gold conjugate fulfilled this requirement.

The close relationship between coated and noncoated pits and their respective vesicular counterparts poses a problem of identifying the free vesicles in sections. The ultimate solution for this problem is analysis of thin serial sections, where surface connections can be discovered or the integrity of vesicular profiles unequivocally documented (40, 54). However, for quantitative studies where a large-scale analysis is necessary, an alternative, less time consuming approach is needed. Hence, we could justify to carry out quantitative analysis of endocytic vesicles on random single sections in our Con A–anti-Con A assay by initially documenting that vesicular profiles containing only the gold label in all cases examined by serial sectioning were truly free vesicles.

It is well established that coated pits and vesicles are pri-

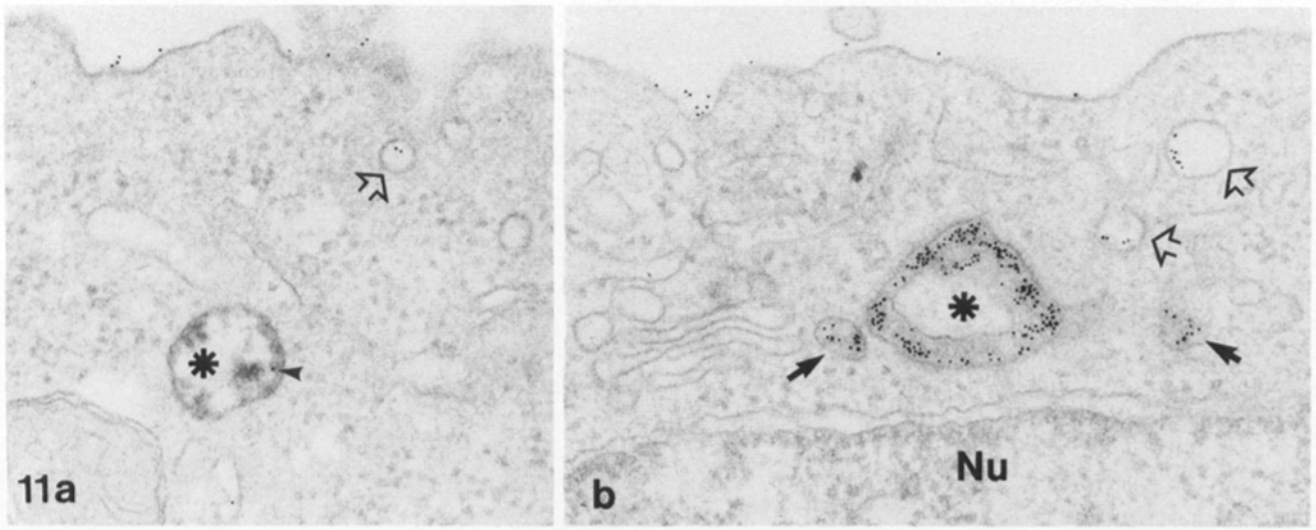

Figure 11. Recycling assay performed by reversing the sequence of the Con A–anti-con A assay. Thus, cells were incubated with anti-Con A–HRP for 15 min at 37°C, then chilled to 4°C, rinsed, and further incubated with Con A–gold for 120 min. Finally, after washing the cells, a chase was performed for 60 s or 15 min at 37°C. (*a*) After a 60-s chase vesicle profiles, either endocytic or surface connected as revealed by their content of the gold marker only (*open arrow*), are found in conjunction with HRP labeled endosomes (*asterisk*) containing no or few gold particles (*arrowhead*). (*b*) After 15-min chase, the HRP-labeled endosomes also contain high numbers of gold particles (*asterisk*). Putative recycling vesicles containing both the gold label and the HRP tag are found (*arrows*) as well as vesicular profiles containing the gold label only (*open arrows*).

marily involved in rapid and efficient (concentrative) uptake of a variety of transmembrane glycoprotein receptors and their physiological ligands (11). Receptor internalization occurs constitutively when the receptors aggregate in coated pits also in the absence of ligands (e.g., LDL and transferrin receptors), or it can be induced by interaction with the ligands (e.g., receptors with tyrosine kinase activity such as the EGF receptor, [4]). On the other hand, clathrin-independent endocytosis seems to be involved in a less efficient, nonconcentrative removal of resident plasma membrane proteins, or proteins that do not have a typical receptor function in ligand uptake (a default pathway of internalization; see references 2, 21). Major histocompatibility (MHC) molecules are of interest here. Thus, Huet et al. (22) reported that MHC class I molecules were internalized via noncoated pits at the plasma membrane, and in a recent study it was found that a small but significant fraction of surface MHC class II molecules is internalized, although the molecules are not present in coated pits (37). Of interest is also a rather large family of proteins that do not cross the membrane lipid bilayer but are rather anchored to membrane glycolipids (phosphotidylinositol-anchored proteins, [PI-P]). These molecules are also excluded from coated pits (1). For instance the PI-P Thy-1, which is excluded from coated pits, is internalized, although very slowly (29). However, an uptake rate of just 5% per hour would make sense in relation to a slow turnover of resident membrane proteins (i.e., proteins not designed for rapid internalization and recycling). Also, immunotoxins bound to Thy-1 are internalized and intoxicate cells (31). Another example of a PI-P is the decay accelerating factor of leucocytes that also seems to be internalized in a clathrin-independent way (50). Membrane glycolipids may also need a slow, continuous internalization, although at least some are excluded from coated pits. For instance, glycolipids with the gal α 1-4 gal structure binding Shiga toxin are excluded from coated pits, unless the toxin is added (48). In addition, several opportunistic ligands of pathophysiological interest use, at least in part, a clathrin-independent mechanism to enter cells (47, 51, 56).

Whereas molecular motors involved in clathrin-dependent endocytosis are well established (see Introduction), much less is known about the possible mechanisms involved in the formation of endocytic vesicles without clathrin. It is known, however, from studies on several cell types that growth factors such as insulin, insulin-like growth factor-I, and EGF as well as the tumor-promoter 12-0-tetradecanoyl-phorbol-13-acetat (TPA) induce membrane ruffling or other changes in surface architecture with a concomitant stimulation of endocytosis, possibly by noncoated vesicles (3, 5, 8, 14, 15, 32, 33, 41, 42, 58). Membrane ruffling involves the cytoskeleton (32, 33, 41, 42) and it is known from several studies that cytoskeletal inhibitors can reduce endocytosis (10, 41–43, 57). Recently we found that cytochalasin D reduces endocytosis of ricin and of the fluid phase marker sucrose without reducing the uptake of transferrin. Moreover, colchicine had a similar effect (46). In contrast to these cytoskeletal inhibitors, EGF and TPA stimulated clathrin-independent endocytosis (46). The noncoated endocytic vesicles analyzed in the present study could thus be formed by constitutive changes in plasma membrane geometry, a kind of ruffling, somehow involving cytoskeletal elements. A detailed study of the effect of EGF and TPA on membrane ruffling and endocytosis using an approach similar to the one reported here might throw more light on these problems.

The identification of two distinct preendosomal vesicle populations raises some important questions in relation to endocytic pathways. Thus, it is unknown whether molecules internalized by the clathrin-independent mechanism described here reach the same endosomal compartment as do molecules such as the transferrin receptor and are subsequently sorted and further transported in the same way, i.e., recycled back to the cell surface, transcytosed, delivered to the *trans*-Golgi network, or directed through a mannose-6-phosphate receptor-enriched prelysosomal compartment to lysosomes (55). Studies by Tran et al. (51) using $\alpha_2$macroglobulin-gold as a marker for coated pit endocytosis and cholera toxin–gold as a marker for smooth pits at the cell surface suggest that molecules taken up by the two mechanisms indeed meet in the same endosomal compartment.

Even though the present findings as well as many previous studies on cultured cells (36, 46, 47, 51) suggest that clathrin-independent endocytosis is a ubiquitous process, future studies will have to determine what the significance of this endocytic mechanism is in various differentiated tissues in the organism.

We wish to thank Marianne Lund, Kirsten Pedersen, Keld Ottosen, Anne-Grethe Myrann, and Jorunn Jacobsen for expert technical assistance. We also thank Dr. Colin Hopkins for providing us with B3/25-gold and Dr. Michael Edidin (Johns Hopkins University, Baltimore, MD) for helpful discussions.

This study was supported by grants from the Danish Cancer Society, the Danish Medical Research Council, the NOVO Foundation, the Leo Nielsen Foundation, the Madsen Foundation, the Wedell-Wedellborgs Foundation, the Gangsted Foundation, the Norwegian Cancer Society, and by a NATO Collaborative Research Grant (CRG 900517).

Received for publication 5 November 1990 and in revised form 24 January 1991.

References

1. Bretscher, M. S., J. N. Thomson, and B. M. F. Pearse. 1980. Coated pits act as molecular filters. *Proc. Natl. Acad. Sci. USA*. 77:4156–4159.
2. Brodsky, F. M. 1988. Living with clathrin: its role in intracellular membrane traffic. *Science (Wash. DC)*. 242:1396–1402.
3. Brunk, U., J. Schellens, and B. Westermark. 1976. Influence of epidermal growth factor (EGF) on ruffling activity, pinocytosis and proliferation of cultivated human glia cells. *Exp. Cell Res.* 103:295–302.
4. Chen, W. S., C. S. Lazar, K. A. Lund, J. B. Welsh, C. P. Chang, G. M. Walton, C. J. Der, H. S. Wiley, G. N. Gill, and M. G. Rosenfeld. 1989. Functional independence of the epidermal growth factor receptor from a domain required for ligand-induced internalization and calcium regulation. *Cell*. 59:33–43.
5. Chinkers, M., J. A. McKanna, and S. Cohen. 1979. Rapid induction of morphological changes in human carcinoma cells A-431 by epidermal growth factor. *J. Cell Biol.* 83:260–265.
6. Ciechanover, A., A. L. Schwartz, A. Dautry-Varsat, and H. F. Lodish. 1983. Kinetics of internalization and recycling of transferrin and the transferrin receptor in a human hepatoma cell line. *J. Biol. Chem.* 258: 9681–9689.
7. Cosson, P., I. de Curtis, J. Pouyssegur, G. Griffiths, and J. Davoust. 1989. Low cytoplasmic pH inhibits endocytosis and transport from the *trans*-Golgi network to the cell surface. *J. Cell Biol.* 108:377–387.
8. Gibbs, E. M., G. E. Lienhard, J. R. Appleman, M. D. Lane, and S. C. Frost. 1986. Insulin stimulates fluid-phase endocytosis and exocytosis in 3T3-L1 adipocytes. *J. Biol. Chem.* 261:3944–3951.
9. Glickman, J. N., E. Conibear, and B. M. F. Pearse. 1989. Specificity of binding of clathrin adaptors to signals on the mannose-6-phosphate/insulin-like growth factor II receptor. *EMBO (Eur. Mol. Biol. Organ.) J.* 8:1041–1047.
10. Goldman, R. 1976. The effect of cytochalasin B and colchicine on concanavalin A induced vacuolation in mouse peritoneal macrophages. *Exp. Cell. Res.* 99:385–394.
11. Goldstein, J. L., M. S. Brown, R. G. W. Anderson, D. W. Russell, and

W. J. Schneider. 1985. Receptor mediated endocytosis: concepts emerging from the LDL receptor system. *Annu. Rev. Cell Biol.* 1:1-39.
12. Gruenberg, J., and K. E. Howell. 1989. Membrane traffic in endocytosis: insights from cell-free assays. *Annu. Rev. Cell Biol.* 5:453-481.
13. Guagliardi, L. E., B. Koppelman, J. S. Blum, M. S. Marks, P. Cresswell, and F. M. Brodsky. 1990. Co-localization of molecules involved in antigen processing and presentation in an early endocytic compartment. *Nature (Lond.).* 343:133-139.
14. Haigler, H. T., J. A. McKanna, and S. Cohen. 1979. Direct visualization of the binding and internalization of a ferritin conjugate of epidermal growth factor in human carcinoma cells A-431. *J. Cell Biol.* 81:382-395.
15. Haigler, H. T., J. A. McKanna, and S. Cohen. 1979. Rapid stimulation of pinocytosis in human carcinoma cells A-431 by epidermal growth factor. *J. Cell Biol.* 83:82-90.
16. Hansen, S. H., O. W. Petersen, K. Sandvig, S. Olsnes, and B. van Deurs. 1989. Internalized ricin and the plasma membrane glycoprotein MAM-6 colocalize in the trans-Golgi network of T47D human breast carcinoma cells. *Exp. Cell Res.* 185:373-386.
17. Heuser, J. 1989. Effects of cytoplasmic acidification on clathrin lattice morphology. *J. Cell Biol.* 108:401-411.
18. Heuser, J. E., and R. G. W. Anderson. 1989. Hypertonic media inhibit receptor-mediated endocytosis by blocking clathrin-coated pit formation. *J. Cell Biol.* 108:389-400.
19. Hopkins, C. R. 1983. Intracellular routing of transferrin and transferrin receptors in epidermoid carcinoma A431 cells. *Cell.* 35:321-330.
20. Hopkins, C. R., and I. S. Trowbridge. 1983. Internalization and processing of transferrin and the transferrin receptor in human carcinoma A431 cells. *J. Cell Biol.* 97:508-521.
21. Hubbard, A. 1989. Endocytosis. *Curr. Opin. Cell Biol.* 1:675-683.
22. Huet, C., J. F. Ash, and S. J. Singer. 1980. The antibody-induced clustering and endocytosis of HLA antigens on cultured human fibroblasts. *Cell.* 21:429-438.
23. Iacopetta, B. J., S. Rothenberger, and L. C. Kühn. 1988. A role for the cytoplasmic domain in transferrin receptor sorting and coated pit formation during endocytosis. *Cell.* 54:485-489.
24. Jing, S., T. Spencer, K. Miller, C. Hopkins, and I. S. Trowbridge. 1990. Role of the human transferrin receptor cytoplasmic domain in endocytosis: localization of a specific sequence for internalization. *J. Cell Biol.* 110:283-294.
25. Kartenbeck, J., H. Stukenbrok, and A. Helenius. 1989. Endocytosis of simian virus 40 into the endoplasmic reticulum. *J. Cell Biol.* 109:2721-2729.
26. Keen, J. H. 1990. Clathrin and associated assembly and disassembly proteins. *Annu. Rev. Biochem.* 59:415-438.
27. Ktistakis, N. T., D. Thomas, and M. G. Roth. 1990. Characteristics of the tyrosine recognition signal for internalization of transmembrane surface glycoproteins. *J. Cell Biol.* 111:1393-1407.
28. Larkin, J. M., M. S. Brown, J. L. Goldstein, and R. G. W. Anderson. 1983. Depletion of intracellular potassium arrests coated pit formation and receptor-mediated endocytosis in fibroblasts. *Cell.* 33:273-285.
29. Lemansky, P., S. H. Fatemi, B. Gorican, S. Meyale, R. Rossero, and A. M. Tartakoff. 1990. Dynamics and longevity of the glycolipid-anchored membrane protein, Thy-1. *J. Cell Biol.* 110:1525-1531.
30. Madshus, I. H., K. Sandvig, S. Olsnes, and B. van Deurs. 1987. Effect of reduced endocytosis induced by hypotonic shock and potassium depletion on the infection of Hep 2 cells by picornaviruses. *J. Cell. Physiol.* 131: 14-22.
31. Marsh, J. W. 1988. Antibody-mediated routing of diphtheria toxin in murine cells results in a highly efficacious immunotoxin. *J. Biol. Chem.* 263: 15993-15999.
32. Miyata, Y., M. Hoshi, S. Koyasu, T. Kadowaki, M. Kasuga, I. Yahara, E. Nishida, and H. Sakai. 1988. Rapid stimulation of fluid-phase endocytosis and exocytosis by insulin, insulin-like growth factor-I, and epidermal growth factor in KB cells. *Exp. Cell Res.* 178:73-83.
33. Miyata, Y., E. Nishida, S. Koyasu, I. Yahara, and H. Sakai. 1989. Regulation by intracellular Ca^{2+} and cyclic AMP of the growth factor-induced ruffling membrane formation and stimulation of fluid-phase endocytosis and exocytosis. *Exp. Cell Res.* 181:454-462.
34. Montesano, R., J. Roth, A. Robert, and L. Orci. 1982. Non-coated membrane invaginations are involved in binding and internalization of cholera and tetanus toxins. *Nature (Lond.).* 296:651-653.
35. Moore, M. S., D. T. Mahaffey, F. M. Brodsky, and R. G. W. Anderson. 1987. Assembly of clathrin-coated pits onto purified plasma membranes. *Science (Wash. DC).* 236:558-563.
36. Moya, M., A. Dautry-Varsat, B. Goud, D. Louvard, and P. Boquet. 1985. Inhibition of coated pit formation in Hep-2 cells blocks the cytotoxicity of diphtheria toxin but not that of ricin toxin. *J. Cell Biol.* 101:548-559.
37. Neefjes, J. J., V. Stollorz, P. J. Peters, H. J. Geuze, and H. L. Ploegh. 1990. The biosynthetic pathway of MHC class II but not class I molecules intersects the endocytic route. *Cell.* 61:171-183.
38. Oka, J. A., M. D. Christensen, and P. H. Weigel. 1989. Hyperosmolarity inhibits galactosyl receptor-mediated but not fluid phase endocytosis in isolated rat hepatocytes. *J. Biol. Chem.* 264:12016-12024.
39. Pearse, B. M. F. 1987. Clathrin and coated vesicles. *EMBO (Eur. Mol. Biol. Organ.) J.* 6:2507-2512.
40. Petersen, O. W., and B. van Deurs. 1983. Serial-section analysis of coated pits and vesicles involved in adsorptive pinocytosis in cultured fibroblasts. *J. Cell Biol.* 96:277-281.
41. Phaire-Washington, L., S. C. Silverstein, and E. Wang. 1980. Phorbol myristate acetate stimulates microtubule and 10-nm filament extension and lysosome redistribution in mouse macrophages. *J. Cell Biol.* 86:641-655.
42. Phaire-Washington, L., E. Wang, and S. Silverstein. 1980. Phorbol myristate acetate stimulates pinocytosis and membrane spreading in mouse peritoneal macrophages. *J. Cell Biol.* 86:634-640.
43. Pratten, M. K., and J. B. LLoyd. 1979. Effects of temperature, metabolic inhibitors and some other factors on fluid-phase and adsorptive pinocytosis by rat peritoneal macrophages. *Biochem. J.* 180:567-571.
44. Rodman, J. S., R. W. Mercer, and P. D. Stahl. 1990. Endocytosis and transcytosis. *Curr. Opin. Cell Biol.* 2:664-672.
45. Rothberg, K. G., Y. Ying, J. F. Kolhouse, B. A. Kamen, and R. G. W. Anderson. 1990. The glycophospholipid-linked folate receptor internalizes folate without entering the clathrin-coated pit endocytic pathway. *J. Cell Biol.* 110:637-649.
46. Sandvig, K., and B. van Deurs. 1990. Selective modulation of the endocytic uptake of ricin and fluid phase markers without alteration in transferrin endocytosis. *J. Biol. Chem.* 265:6382-6388.
47. Sandvig, K., S. Olsnes, O. W. Petersen, and B. van Deurs. 1987. Acidification of the cytosol inhibits endocytosis from coated pits. *J. Cell Biol.* 105:679-689.
48. Sandvig, K., S. Olsnes, J. E. Brown, O. W. Petersen, and B. van Deurs. 1989. Endocytosis from coated pits of Shiga toxin: a glycolipid-binding protein from *Shigella dysenteriae 1*. *J. Cell Biol.* 108:1331-1343.
49. Sandvig, K., S. Olsnes, O. W. Petersen, and B. van Deurs. 1989. Control of coated-pit function by cytoplasmic pH. *Methods Cell Biol.* 32:365-382.
50. Tausk, F., M. Fey, and I. Gigli. 1989. Endocytosis and shedding of the decay accelerating factor on human polymorphonuclear cells. *J. Immunol.* 143:3295-3302.
51. Tran, D., J.-L. Carpentier, F. Sawano, P. Gordon, and L. Orci. 1987. Ligands internalized through coated or noncoated invaginations follow a common intracellular pathway. *Proc. Natl. Acad. Sci. USA* 84:7957-7961.
52. Ullrich, A., and J. Schlessinger. 1990. Signal transduction by receptors with tyrosine kinase activity. *Cell.* 61:203-212.
53. van Deurs, B., and K. Nilausen. 1982. Pinocytosis in mouse L-fibroblasts: ultrastructural evidence for a direct membrane shuttle between the plasma membrane and the lysosomal compartment. *J. Cell Biol.* 94:279-286.
54. van Deurs, B., O. W. Petersen, and M. Bundgaard. 1983. Do coated pinocytic vesicles exist? *Trends Biochem. Sci.* 8:400-401.
55. van Deurs, B., O. W. Petersen, S. Olsnes, and K. Sandvig. 1989. The ways of endocytosis. *Int. Rev. Cytol.* 117:131-177.
56. van Deurs, B., K. Sandvig, O. W. Petersen, and S. Olsnes. 1990. Endocytosis and intracellular sorting of ricin. *In* Trafficking of Bacterial Toxins. C. B. Saelinger, editor. CRC Press, Inc., Boca Raton, FL. 91-119.
57. Wagner, R., M. Rosenberg, and R. Estensen. 1971. Endocytosis in chang liver cells. Quantitation by sucrose-^{3}H uptake and inhibition by cytochalasin B. *J. Cell Biol.* 50:804-817.
58. West, M. A., M. S. Bretscher, and C. Watts. 1989. Distinct endocytotic pathways in epidermal growth factor-stimulated human carcinoma A431 cells. *J. Cell Biol.* 109:2731-2739.